

Fabrication of trench nanostructures for extreme ultraviolet lithography masks by atomic force microscope lithography

Gwangmin Kwon, Kyeongkeun Ko, Haiwon Lee, Woongsun Lim, Geun Young Yeom, Sunwoo Lee, and Jinho Ahn

Citation: *Journal of Vacuum Science & Technology B, Nanotechnology and Microelectronics: Materials, Processing, Measurement, and Phenomena* **29**, 011034 (2011);

View online: <https://doi.org/10.1116/1.3534025>

View Table of Contents: <http://avs.scitation.org/toc/jvb/29/1>

Published by the [American Vacuum Society](#)

HIDEN
ANALYTICAL

Instruments for Advanced Science

Contact Hiden Analytical for further details:

W www.HidenAnalytical.com
E info@hiden.co.uk

CLICK TO VIEW our product catalogue



Gas Analysis

- dynamic measurement of reaction gas streams
- catalysis and thermal analysis
- molecular beam studies
- dissolved species probes
- fermentation, environmental and ecological studies



Surface Science

- UHV TPD
- SIMS
- end point detection in ion beam etch
- elemental imaging - surface mapping



Plasma Diagnostics

- plasma source characterization
- etch and deposition process reaction kinetic studies
- analysis of neutral and radical species



Vacuum Analysis

- partial pressure measurement and control of process gases
- reactive sputter process control
- vacuum diagnostics
- vacuum coating process monitoring

Fabrication of trench nanostructures for extreme ultraviolet lithography masks by atomic force microscope lithography

Gwangmin Kwon and Kyeongkeun Ko

Department of Nanotechnology, Hanyang University, Seoul 133-791, Korea

Haiwon Lee^{a)}

Department of Chemistry, Hanyang University, Seoul 133-791, Korea

Woongsun Lim and Geun Young Yeom

Department of Material Science and Engineering, Sungkyunkwan University, Suwon 440-746, Korea

Sunwoo Lee and Jinho Ahn

Department of Material Science and Engineering, Hanyang University, Seoul 133-791, South Korea

(Received 28 June 2010; accepted 13 December 2010; published 25 January 2011)

We describe methods to fabricate extreme ultraviolet lithography (EUVL) absorber mask patterns by atomic force microscope (AFM) lithography and inductively coupled plasma (ICP) etching. AFM lithography, based on anodization and cross-linking polymer resist, was applied to fabricate trench structures using only Ta and Cr/Ta bilayers. In particular, the top Cr layer was used not only as a hard mask to etch the underlying Ta in dry-etching, but also as an absorber material together with Ta. The Cr oxide or Ta with respect to Cr was eliminated due to the clear etch-selectivity of ICP dry-etching using C_4F_8 gas. This is a simple fabrication technique using AFM lithography fabricated metal trenches for the production of isolated metal structures as well as for producing EUVL absorber patterns. © 2011 American Vacuum Society. [DOI: 10.1116/1.3534025]

I. INTRODUCTION

When the limits of optical lithography were reached, the next generation of lithography, extreme ultraviolet lithography (EUVL) using a 13.5 nm wavelength, became a topic of study. EUVL studies began in the mid-1980s in an attempt to overcome the resolution limits of optical lithography. Further developments, such as EUV source, reflective EUV mask, resist and EUV equipment necessary for the application of EUV lithography in semiconductor manufacturing have been carried out.¹ In particular, the EUV mask was identified as an important component necessary for achieving critical dimension control below 32 nm minimum feature size for semiconductor devices. The characterization of EUV masks has been largely dependent on both absorber material and the reflective multilayer structure that must be defect-free down to the nanometer scale. Various absorber materials such as Al-Cu, Ti, TiN, Ta, TaN, and Cr have been proposed,² and electron beam lithography based on the standard photomask tool has been employed.³ In this report, we introduce EUVL mask fabrication procedures using atomic force microscope (AFM) lithography which offers advantages such as high resolution, low cost, low energy, and easy fabrication of critical patterns.^{4,5} This lithographic technique is based on electrochemical oxidation of an anodic substrate such as Al, Cr, GaAs, Si, Ta, and Ti,⁶⁻¹¹ electrochemically modifying organic materials,¹²⁻¹⁵ directly transferring molecular species¹⁶ and mechanically engraving soft layers.¹⁷ In order to fabricate metal structures in nanoscale by using AFM lithography,

some researchers have introduced methods including a lift-off process using a metal/polymer bilayer resists¹⁸ and transferring an amorphous carbon mask onto a metal with an Ar ion etching process.¹⁹ Here, in order to fabricate Ta trench structures, Ta was direct anodized and selectively patterned by AFM lithography and inductively coupled plasma (ICP) dry-etching, respectively. In order to overcome the depth limit of trench in a mask fabrication process based on a transferring method with increased etching selectivity, we used the Cr and Ta bilayers as a mask and an absorber metal, respectively. The Cr was employed as absorber material, as well as a hard metal mask, due to its high dry etch resistance.²⁰⁻²⁶ In order to make Cr mask patterns, a polymer nanopatterning procedure used in AFM electron-induced lithography was applied to pattern a clear field Cr mask onto Ta. The synthesized polymer resist containing a photoacid generator (PAG) was electrochemically cross-linked by AFM electron-induced lithography.²⁷ The negative type resist pattern served as a hard mask to wet-etch the Cr. For patterning a dark field Cr mask, the Cr was anodized by AFM lithography and then the Cr oxide was etched by ICP dry-etching. Cr is a well known anodic material that possesses higher electrical and thermal conductivities than Ta, Ti, and Si (Ref. 28) for AFM anodization lithography. All of the above patterned Cr masks were sequentially transferred into the underlying Ta by ICP dry-etching. These lithographic and etching procedures may be effectively and widely applied to fabricate metal trench structures not only for production of EUV masks but also for production of nanoscale metal structures for templates and devices.

^{a)}Electronic mail: haiwon@hanyang.ac.kr

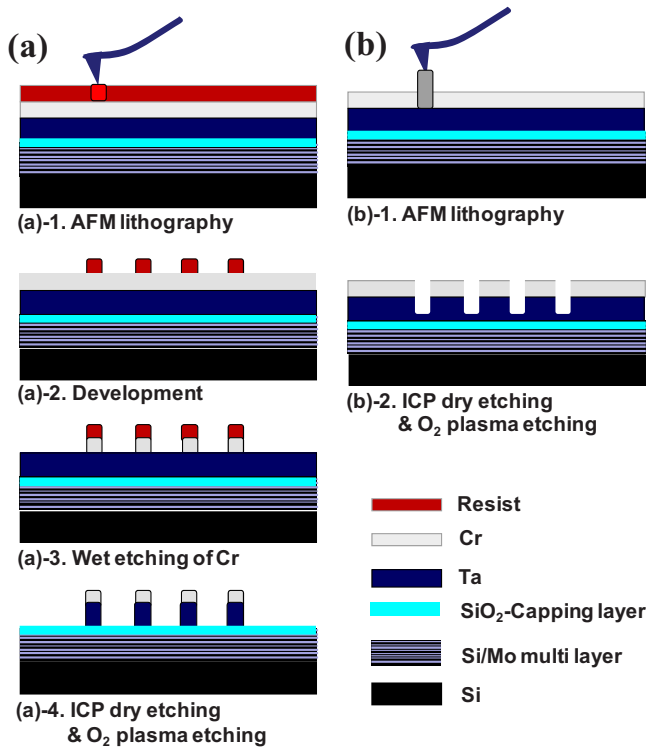


FIG. 1. (Color online) Procedures for patterning trench structures by selectively etching (a) Ta and Cr masks by a cross-linked polymer resist masking process, and (b) Cr and Cr oxide/Ta by AFM based lithography.

II. EXPERIMENT

A. Fabrication of trench structures using anodized Ta_2O_5 on Ta

AFM lithography was carried out on the Ta layer on Mo/Si multilayer film structures atop bare Si (100) wafers ($\rho \sim 10\text{--}20 \text{ } \Omega \text{ cm}$, Silicon Technology, Japan). Ta was deposited at 30 W dc bias power and 0.5 mtorr working pressure using a magnetron sputtering system (LAMS-045CL, IDT Engineering, Korea). Anodization and surface imaging were performed by AFM (XE-100, Park Systems, Korea) using a metal coated silicon tip (NSC36/Ti-Pt, force constant 0.6 N/m, MikroMasch, USA) in contact mode. Ta_2O_5 line patterns were fabricated at a negative tip bias of -10 V at a speed of $5 \text{ } \mu\text{m/s}$. The relative humidity and temperature during lithography were 50% and $25 \text{ } ^\circ\text{C}$, respectively. The anodized Ta_2O_5 patterns were etched onto a Ta layer using ICP dry-etching at a working pressure of 10 mtorr, RF power of 600 W, and C_4F_8 gas flow of 11 sccm for 50 s.

B. Fabrication of trench structures using a Cr metal mask

The Cr/Ta bilayer was used to fabricate deep absorber trench structures. Ta and Cr with thickness of 60 and 5 nm, respectively, were prepared by magnetron sputtering system. Two lithographic techniques were used to fabricate Cr metal masks onto a Ta substrate. In the first method, the cross-linked resist patterns of the mask were formed by AFM lithography, as shown in Fig. 1(a). The polymer resist contain-

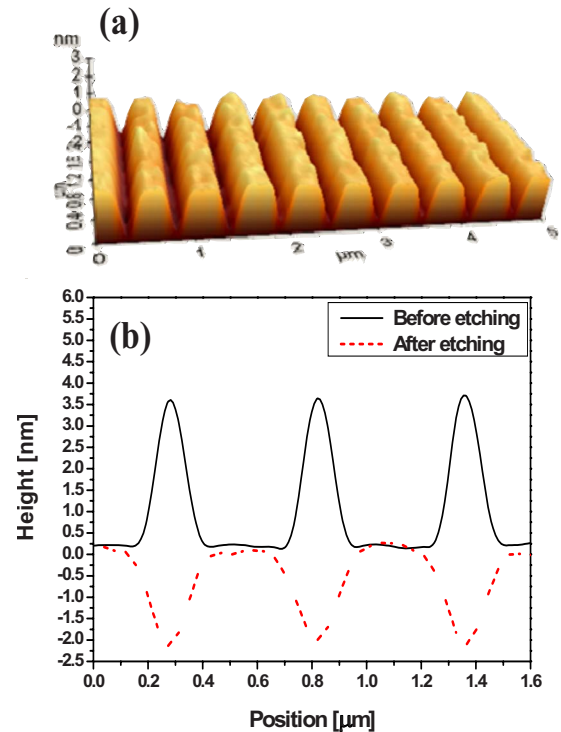


FIG. 2. (Color online) (a) AFM three-dimensional image of Ta_2O_5 anodized by AFM lithography (b) matching cross section profile before and after etching of Ta_2O_5 (depth: 2 nm, FWHM: 150 nm).

ing a PAG was synthesized by free radical polymerization in tetrahydrofuran (THF) using azobisisobutyronitrile (AIBN) and included a 36% PAG unit attached to PMMA as a pendent group. The 1.5 wt % by weight polymer solution (0.15 g/10 mL) in DMF was coated at 4000 rpm for 40 s and prebaked at $100 \text{ } ^\circ\text{C}$ for 1 min. The film was then cross-linked by a positive bias of 5 V applied from the Pt coated silicon tip at a speed of $5 \text{ } \mu\text{m/s}$ in contact mode. Postexposure baking was carried out at $120 \text{ } ^\circ\text{C}$ for 2 min and then the resist was developed with IPA/DI water (7:3). The formed resist patterns played the role of mask to etch the Cr using wet-etchant (Cyantek Corporation, U.S.A.); the fabricated Cr patterns then acted as a mask to etch the underlying Ta using ICP dry-etching under a working pressure of 10 mtorr, RF power of 500 W, and C_4F_8 gas flow of 11 sccm for 5 min. In the second procedure, using a Cr/Ta bilayer as shown in Fig. 1(b), the top Cr layer was anodized by AFM anodization lithography at a negative tip bias of -6 V at a speed of $5 \text{ } \mu\text{m/s}$. The fabricated Cr oxide and Ta have high etch selectivities with respect to the Cr. To etch the Cr oxide and the underlying Ta, the ICP dry-etching process was sequentially carried out under a working pressure of 10 mtorr, RF power of 500 W, and C_4F_8 gas flow of 11 sccm for 15 min.

III. RESULTS AND DISCUSSION

Figure 2 shows Ta line patterns fabricated using AFM lithography before and after dry-etching of Ta_2O_5 line patterns formed by AFM anodization lithography. Preferentially, lithographic nanostructures have a line height of $\sim 4 \text{ nm}$ and

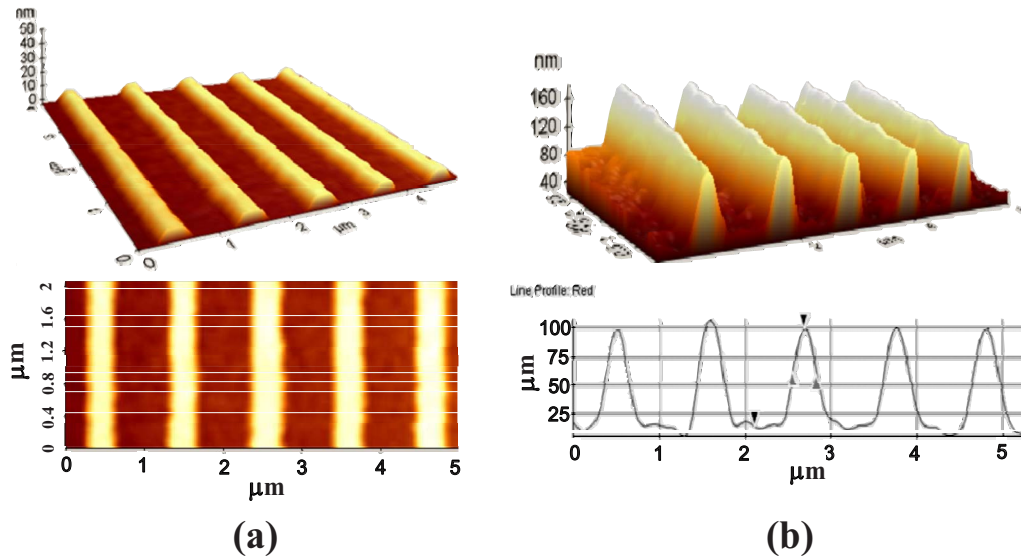


FIG. 3. (Color online) (a) Negative PAG-containing polymer resist patterns (height: 8.3 nm, FWHM: 290 nm), (b) Cr/Ta line structures using etching of Cr and Ta by wet-etching and ICP dry-etching, respectively (height: 85 nm, FWHM: 270 nm).

a full width half maximum (FWHM) of ~ 100 nm. The Ta trench structures had a depth of 2 nm and a FWHM of 150 nm after dry-etching. Ta₂O₅ nanostructures were etched in the range of ~ 6.5 nm in the vertical direction and ~ 10 nm in the horizontal direction. As illustrated in the experimental results, direct metal-oxide (Ta-O) etching without the use of a shadow mask, following AFM lithography, has significant limitations for the manufacture of Ta fine patterns because of the low selectivity between Ta and Ta₂O₅ materials during etching. In order to increase the depth of Ta trench structures, the fabrication process requires the use of hard mask material with high Ta etch-selectivity.

We suggested that Cr would act as a useful metal mask to pattern the underlying Ta. In order to confirm the etch characteristics and selectivity of Cr and Ta in ICP dry-etching, two samples were deposited onto Cr and Ta and patterned by photolithography with conventional photo resists (polymethylmethacrylate, PMMA). In the case of the Cr surface, Cr had a strong etch resistance in the fluorocarbon plasma during ICP dry-etching with C₄F₈ gas at 10 mTorr and 500 W. The fluorine radical from the C₄F₈ gas plasma was reacted with Cr for 7 min and a small amount of volatile by-product CrF_n and nonvolatile by-product carbon polymer with about a 2 nm thickness were generated. The carbon polymer that was lightly deposited by physical-adsorption onto the Cr surface during the etching process is known to be helpful in reducing the charge effect.²⁹ This carbon polymer deposition may also be a crucial factor in improving etch-selectivity with respect to an etched material. After the etching process, the deposited carbon film was removed by an O₂ plasma ashing process.²⁹ In comparison, Ta was easily etched, under the same conditions, with an etch rate of 20 nm/min, by the generation of the volatile by-product TaF_n without the need for neutral carbon species. In order to fabricate Cr/Ta trench structures, we used the PAG-containing resist film to wet-etch a Cr mask onto the Ta. The coated resists on the Cr/Ta

layer were electrically and thermally exposed by AFM lithography and then developed in IPA/DI water (7:3). The cross-linked negative polymer resist was fabricated using AFM lithography as shown in Fig. 3(a).³⁰ The resist patterns were transferred onto Cr by a wet-etching process. The fabricated Cr patterns were employed as a metal mask to etch the underlying Ta layer using ICP etching with C₄F₈ gas for 5 min. After the dry-etching process, the residue materials were removed by O₂ plasma ashing. Figure 3(b) shows the results of the clear field Cr/Ta mask patterns with 270 nm FWHM and 85 nm height. The thickness of the absorber structures was sufficient to act as an EUV mask.¹ However, the line-width of the structures and the line-edge roughness were somewhat large and rough because of an inadequately defined feature of the wet-etching process with an isotropic undercut characteristic. Figure 4 shows Cr/Ta trench structures fabricated by AFM anodization lithography without a resist mask in a wet-etching process. Cr oxide patterns obtained by AFM lithography on a Cr/Ta layer were eliminated by ICP etching and the grooved Cr patterns acted as a dark field metal mask to etch the underlying Ta. Similarly, Ta was etched after etching off Cr oxide. The local oxidation of a whole Cr layer and a little Ta layer through the control of lithographic conditions is very important in defining the critical dimensions of a mask and for making narrow trench patterns in the etching process. Therefore, in order to minimize Ta oxidation, the appropriate input bias to mainly anodize a Cr layer should be controlled. If both Ta and Cr are widely oxidized by applying a higher one than necessary input bias, the width of the trenches will be increased. The height and FWHM of CrO₃ were 16 and 110 nm, respectively. It was assumed that the metal oxide (MO_n) of AFM lithography was grown with an approximate ratio of 3:1 for upward and downward MO_n growth.^{31,32} The thin 5 nm Cr layer was fully anodized to CrO₃. The CrO₃ nanostructures occurring

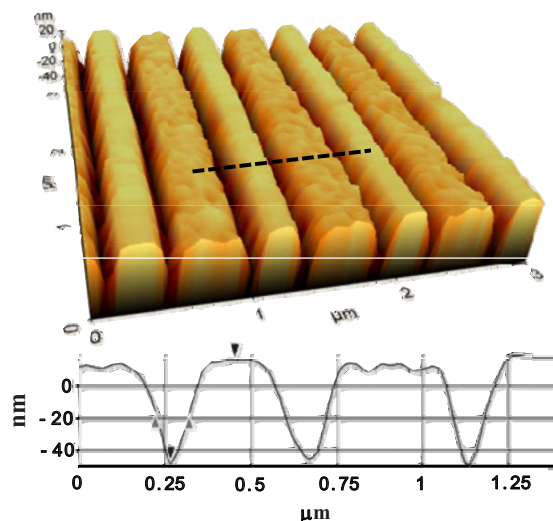


FIG. 4. (Color online) Cr/Ta trench structures produced by basic AFM anodization lithography and dry-etching of CrO_3 and Ta (depth: 67, FWHM: 100 nm).

at the Cr-Ta interface and the underlying Ta layer were selectively and sequentially etched using C_4F_8 gas plasma for 15 min as shown in Fig. 4. The average FWHM and depth of Cr/Ta trench patterns were 100 nm and 67 nm (aspect ratio = 0.67), respectively. According to the above described processes of Cr/Ta bilayer trench structure fabrication, the Cr metal mask gave a high etch-selectivity for the underlying Ta etching. The reflected image of a mask will be projected through $4\times$ reduction optics in an EUVL system. Therefore, the size of exposed features will be smaller than 30 nm. The fabricated trench patterns show slight edge roughness and surface roughness ($R_a=3.2$ nm) due to metal grain size (average diameter=50 nm) in the patterned Cr etch mask. The further optimization of a wet- or dry-etching process along with an AFM electrochemical lithographic process using a cross-linked polymer resist or a bare anodic metal substrate may improve line edge roughness and produce adequate features.

IV. CONCLUSION

We demonstrated various metal trench fabrication methods based on polymer resist cross-linking and anodization by simple AFM electrochemical lithography with an ICP dry-etching process using C_4F_8 gas. Our fabrication method, using a Cr hard mask to pattern the underlying Ta as an EUV absorber metal, was able to overcome the limit of etch depth in the anodized Ta etching process. The Cr patterned using novel PAG-containing polymer resists acted as a light field metal mask to etch Ta. Also, in the case of a direct Cr anodization by AFM lithography onto the Cr/Ta bilayer, Cr/Ta trench patterns were simply and sequentially fabricated by transferring the grooved Cr onto the underlying Ta. These methods can be used to fabricate features in the making of isolated metal trench structures and the well defined features will be acceptable for the intended application like EUV absorber masks.

ACKNOWLEDGMENTS

This work was supported by the National Program for Tera-level Nanodevices (TND), the International Research & Development Program of the National Research Foundation of Korea (NRF) funded by the Ministry of Education, Science and Technology (MEST) of Korea (Grant No. K20901000006-09E0100-00610), the Seoul R&D Program (10919), the Korea Foundation for International Cooperation of Science and Technology (KICOS), and the research fund of Hanyang University (HYU-2011-T).

- ¹P. J. Silverman, *J. Microlithogr., Microfabr., Microsyst.* **4**, 011006 (2005).
- ²P. Yan, G. Zhang, A. Ma, and T. Liang, *Proc. SPIE* **4343**, 409 (2001).
- ³G. Zhang, P. Yan, T. Liang, Y. Du, P. Sanchez, S. Park, E. J. Lanzendorf, C. J. Choi, E. Y. Shu, A. R. Stivers, J. Farnsworth, K. Hsia, M. Chandhok, M. J. Leeson, and G. Vandentop, *Proc. SPIE* **6283**, 62830G (2006).
- ⁴S. C. Minne, H. T. Soh, Ph. Flueckiger, and C. F. Quate, *Appl. Phys. Lett.* **66**, 703 (1995).
- ⁵P. A. Fontaine, E. Dubois, and D. Stievenard, *J. Appl. Phys.* **84**, 1776 (1998).
- ⁶H. Sugimura, T. Uchida, N. Kitamura, and H. Masuhara, *Appl. Phys. Lett.* **63**, 1288 (1993).
- ⁷S. Lee, H. Lee, B. Park, and G. Y. Yeom, *Nanotechnology* **16**, 3137 (2005).
- ⁸D. V. Sheglov, A. V. Latyshev, and A. L. Aseev, *Appl. Surf. Sci.* **243**, 138 (2005).
- ⁹E. S. Snow, D. Park, and P. M. Campbell, *Appl. Phys. Lett.* **69**, 269 (1996).
- ¹⁰H. J. Song, M. J. Rack, K. Abugharbieh, S. Y. Lee, V. Khan, D. K. Ferry, and D. R. Allee, *J. Vac. Sci. Technol. B* **12**, 3720 (1994).
- ¹¹Y. Kim, J. Zhao, and K. Uosakia, *J. Appl. Phys.* **94**, 7733 (2003).
- ¹²X. N. Xie, H. J. Chung, C. H. Sow, A. A. Bettiol, and A. T. S. Wee, *Adv. Mater. (Weinheim, Ger.)* **17**, 1386 (2005).
- ¹³W. Lee, H. Lee, and M. Chun, *Langmuir* **21**, 8839 (2005).
- ¹⁴H. Sugimura and N. Nakagiri, *Langmuir* **11**, 3623 (1995).
- ¹⁵S. J. Ahn, Y. K. Jang, H. Lee, and H. Lee, *Appl. Phys. Lett.* **80**, 2592 (2002).
- ¹⁶L. M. Demers, D. S. Ginger, S.-J. Park, Z. Li, S.-W. Chung, and C. A. Mirkin, *Science* **296**, 1836 (2002).
- ¹⁷V. Bouchiat and D. Esteve, *Appl. Phys. Lett.* **69**, 3098 (1996).
- ¹⁸M. Rolandi, C. F. Quate, and H. Dai, *Adv. Mater. (Weinheim, Ger.)* **14**, 191 (2002).
- ¹⁹T. Mühl, H. Brückl, D. Kraut, J. Kretz, I. Mönch, and G. Reiss, *J. Vac. Sci. Technol. B* **16**, 3879 (1998).
- ²⁰S. W. Pang, T. Tamanura, M. Nakao, A. Ozawa, and H. Masuda, *J. Vac. Sci. Technol. B* **16**, 1145 (1998).
- ²¹H. Toshiyoshi and H. Fujita, *J. Microelectromech. Syst.* **5**, 231 (1996).
- ²²K. H. Smith, J. R. Wasson, P. J. S. Mangat, W. J. Dauksher, and D. J. Resnick, *J. Vac. Sci. Technol. B* **19**, 2906 (2001).
- ²³S. Hu, A. Hamidi, S. Altmeyer, T. Koster, B. Spangenberg, and H. Kurz, *J. Vac. Sci. Technol. B* **16**, 2822 (1998).
- ²⁴P. J. S. Mangat, S. D. Hector, M. A. Thompson, W. J. Dauksher, J. Cobb, K. D. Cummings, D. P. Mancini, D. J. Resnick, G. Cardinale, C. Henderson, P. Kearney, and M. Wedowski, *J. Vac. Sci. Technol. B* **17**, 3029 (1999).
- ²⁵C. W. Jurgensen, R. R. Kola, A. E. Novembre, W. W. Tai, J. Frackowiak, L. E. Trimble, and G. K. Celler, *J. Vac. Sci. Technol. B* **9**, 3280 (1991).
- ²⁶A. P. Milenin, C. Jamois, T. Geppert, U. Gosele, and R. B. Wehrspohn, *Microelectron. Eng.* **81**, 15 (2005).
- ²⁷H. Lee, H. Oh, H. Yoon, and Y. Kim, U.S. Patent No. 11/632358 (30 August 2007).
- ²⁸S. Lee, E. Pyo, J. O. Kim, J. Noh, H. Lee, and J. Ahn, *J. Appl. Phys.* **101**, 044905 (2007).

- ²⁹T. Shimmura, Y. Suzuki, S. Soda, S. Samukawa, M. Koyanagi, and K. Hane, *J. Vac. Sci. Technol. A* **22**, 433 (2004).
- ³⁰G. Kwon, S. Kim, M. Jeong, S. Han, C. Choi, S. Han, J. Hong, and H. Lee, *Ultramicroscopy* **109**, 1052 (2009).
- ³¹H. J. Chung, X. N. Xie, C. H. Sow, and A. T. S. Wee, *J. Appl. Phys.* **99**, 044301 (2006).
- ³²C. R. Kinser, M. J. Schmitz, and M. C. Hersam, *Adv. Mater. (Weinheim, Ger.)* **18**, 1377 (2006).